Available online at http://www.journalijdr.com

IJDR

International Journal of Development Research
Vol. 14, Issue, 08, pp. 66399-66404, August, 2024
https://doi.org/10.37118/ijdr.28605.08.2024

ISSN: 2230-9926

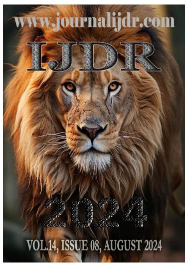

RESEARCH ARTICLE

OPEN ACCESS

OCCURRENCE OF IONOSPHERIC SCINTILLATION DURING ST. PATRICK'S DAY STORM 17 MARCH 2015

***Dr. Purushottam Bhawre**

Assistant Professor, Department of Physics, Rani Durgawati Govt P G College Mandla MP India

ARTICLE INFO

Article History:
Received 17th May, 2024
Received in revised form
20th June, 2024
Accepted 14th July, 2024
Published online 30th August, 2024

Key Words:

Geomagnetic Storm, Ionospheric Scintillation, Amplitude Scintillation, Phase Scintillation.

Corresponding Author:
Dr. Purushottam Bhawre,

ABSTRACT

The Ionospheric scintillation has a huge impact on radio propagation and electronic system performance, thus is substantially studied currently. The particular influence of scintillation on Global Navigation Satellite System (GNSS) is very evident, making GNSS a powerful medium to analyze characteristics of scintillation. Ionospheric scintillation differs in relationship with provisional, provisory and spatial distribution**.** Present study describing about the occurrence of ionospheric scintillation during the geomagnetic storm on 17 March 2015 over Darwin, Australia.1. The sudden storm commencement (SSC) was a quick drop of the SYM-H index to the value of −226 nT. The planetary index of the geomagnetic activity Kp reached the maximum value. During the main phase of the storm (17 March), the interplanetary magnetic field (IMF) orientation displayed a highly complex behavior. The occurrence of phase scintillation activities was high before the storm period as compare with amplitude scintillation. During the strom period scintillation activities were noticed very low.

Citation**:** ***Dr. Purushottam Bhawre. 2024.*** *"Occurrence of ionospheric scintillation during st. patrick's day storm 17 march 2015". International Journal of Development Research*, 14, (08), 66399-66404.

INTRODUCTION

Scintillations occur when electromagnetic waves traverse scintillations occur when electromagnetic waves traverse a region of irregularities containing fluctuations within the index of refraction and may cause a signal's amplitude or phase to fluctuate concerning its mean level as a result of the signal's electromagnetic energy is scattered and decentralized by the disturbed ionospheric region. Before coming into the region of irregularities the electromagnetic radiation possesses a front of constant section. when exiting the region of irregularities the previously constant section front varies in section, depending on the character of the index of refraction irregularities. [8] The prevalence of scintillations has been studied for several decades and its morphology has been documented extensively for the auroral, midlatitude and equatorial regions [Aarons, 1977, 1982]. The foremost intense scintillations have been discovered within the nighttime equatorial region. [9] The ionospheric irregularities inflicting the scintillations are perpetually in motion, thanks to the presence of neutral air winds and electrical and magnetic fields. The drift rate of the irregularities may be calculable from the time lags of the scintillations discovered with many receivers at spaced intervals [Valladares et al., 1996; Kil et al., 2000; Kintner and Ledvina, 2004]. Through spaced receiver and incoherent backscatter techniques, the equatorial irregularities have been found to drift within the within the direction, with a vertical part of drift gift in addition [Woodman, 1970; Paulson, 1984]. The drift velocities simply when native sunset might vary significantly from the postmidnight velocities.

The major impact of ionospheric scintillation on GNSS (Global Navigation Satellite System) will be roughly divided into 2 classes [2–6]. Firstly, it most likely causes a severe decrease in amplitude leading to cycle slips, or maybe an entire loss of lock to satellite signals for GNSS receivers. Secondly, the speedy fluctuation on part could end in a rise of following loop errors. The threat caused by ionospheric scintillation is non-ignorable. However, the distorted signals conversely offer a medium to check and model the region. Some changed GNSS receivers were thus used to observe the event of scintillation, like ionospheric scintillation monitors (ISMs) [7], etc. Extensive studies are administrated on ionospheric scintillation. The severest ionospheric scintillation typically happens at low latitudes attributable to the impact of Rayleigh–Taylor instabilityaround equatorial region. A few sectors around Far eastern Asia have already been widely focused on and studied, taking the geomagnetic surprise influence into consideration [8]. It really is broadly accepted that scintillation is closely related to the behavior of plasma pockets, which has already been deeply looked into during storm time at middle latitudes [9]. This research sheds light on particularities of local characteristics of scintillation and its inner physical mechanism may be determined by several factors thoroughly. Researchers [10] have analyzed the scintillation characteristics and scintillation results on Global Placement System (GPS), dependent on the data sets collected in July and Aug 2012 in Hong Kong. The impact of scintillation on GPS signals has also been analyzed in European Frosty from 8 to 14 November 2005 [11]. Within addition, researchers at Stanford University looked into aviation GNSS performance under ionospheric scintillation [2]. On the other hand, those previous studies were integrated with a limited variety of observations, and some focus too much on the data during solar maximum or geomagnetic thunder or wind storms. Present study describing about the occurrence of ionospheric scintillation during the geomagnetic storm on 17 March 2015 over Darwin, Australia.

Data and Estimation Technique: GPS data that is available freely in the Space Weather Services (SWS) website, www.sws.bom.gov.au, was downloaded for January 2020 to April 2021. Darwin Australia was chosen as an area of interest. This data was extracted using zip applications and the data analyzed for presence of S4 and sigma60 values. After downloading the data, Gnuplot has been used to produce different graphs comparing variations expected in the ionospheric scintillations. Single graphs for amplitude scintillations S4 were plotted separately. The data for sigma60 were also plotted on different graphs.

Amplitude Scintillation: The GISTM used in this analysis measures both amplitude and phase scintillation. Amplitude scintillation is defined by the S_4 index that is derived from detrained intensities of signals received from satellites. The S_4 index is computed over 60-second intervals and stored in the Ionospheric Scintillation Monitor Receiver (GISM) data log along with the phase measurements. This is referred to as the Total S_4 (or S_{4T}). The normalized S_4 index, including the effects of ambient noise, is defined as follows:

$$S_{4T} = \sqrt{\frac{\langle P^2 \rangle - \langle P \rangle^2}{\langle P \rangle^2}} \qquad \ldots\ldots\ldots\ldots\ldots\ldots\ldots\ldots 1$$

The amplitude measurements are filtered using a Low Pass Filter (LPF) and the effects of ambient noise removed from the S_{4T}. This is achieved by estimating the average signal-to-noise ratio over the 60-second interval. The 60-second estimates are then used to determine the expected S_4 correction (or S_{4N_o}) due to ambient noise. The use of this average signal-to-noise ratio (S/N_o) is feasible because the amplitude scintillation fades do not significantly alter the S/N_o. Knowing the S/N_o, S_{4N_o} due to ambient noise becomes:

$$S_{4N_o} = \sqrt{\frac{100}{S/N_o}\left[1 + \frac{500}{19S/N_o}\right]} \qquad \ldots\ldots\ldots\ldots\ldots\ldots\ldots\ldots 2$$

Equation 2 is referred to as the S_4 correction (or S_{4N_o}). By subtracting the square of the right hand side of Equation 2 from the square of the right hand side of Equation 1, and replacing the S/N_o with the 60-second estimates. Equation 1 may be modified to give the S_4 index, with the effects of ambient noise removed, as follows:

$$S_4 = \sqrt{\frac{\langle P^2 \rangle - \langle P \rangle^2}{\langle P \rangle^2} - \frac{100}{S/N_o}\left[1 + \frac{500}{19S/N_o}\right]} \qquad \ldots\ldots\ldots\ldots\ldots\ldots\ldots\ldots 3$$

RESULTS

Geomagnetic Condition: Geomagnetic condition we are describing in figure 2.The severe geomagnetic storm occurred on 17 March 2015 and caused the dramatic response in the ionosphere–plasmasphere–magnetosphere system. The sudden storm commencement (SSC) was registered at ~0445 UT and then there was a quick drop of the SYM-H index to the value of −226 nT, observed at ~2300 UT, with a couple of local minima of −93 and −164 nT at ~0940 and ~1740 UT respectively (Fig. 1). The planetary index of the geomagnetic activity Kp reached the maximum value of 8 after ~12 UT on 17 March 2015, qualifying it as a severe geomagnetic storm.During the main phase of the storm (17 March), the interplanetary magnetic field (IMF) orientation displayed a highly complex behavior. Three IMF components (top panels of Fig. 1) switched several times from positive to negative values and vice versa. Right after the shock arrival, the northward IMF Bz component reached the value of about 25 nT. At ~0530 UT the IMF Bz turned southward and reached the first minimal value of −18 nT at 0615 UT.

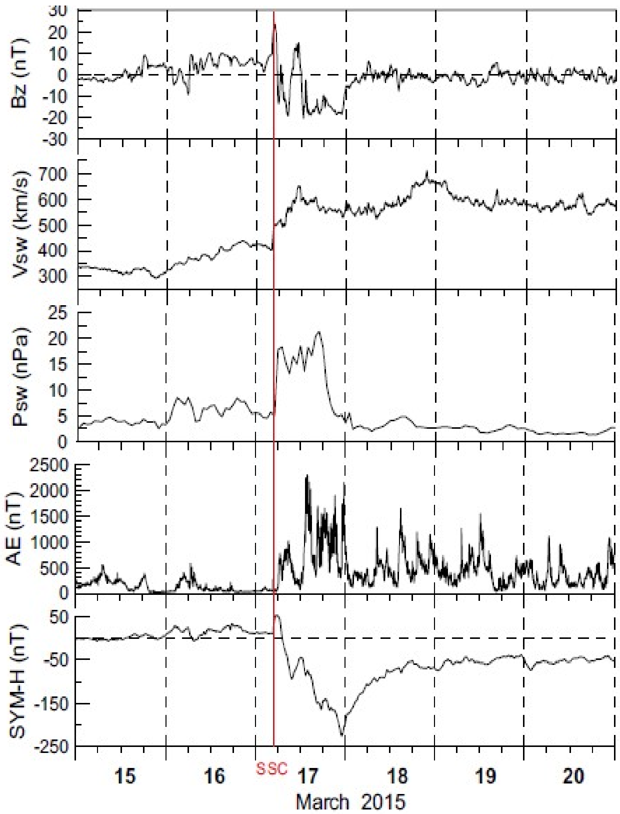

Figure 1. Geomagnetic condition during the St. Patrick's Day storm 17 march 2015

Then the IMF Bz sharply turned northward and varied significantly between north and south during ~8 h. After ~1340 UT the Bz turned southward again and remained south till the end of this day. From ~06 till 11 UT, there are observed dominating positive Bx and negative By with peak values of 16.5 and −16.8 nT for Bx and By, respectively. During 11–15 UT with the new southward turning of Bz, the opposite situation with Bx/By domination occurred—Bx became negative with the minimal values of −14 nT while By component became positive with the peak of 30 nT. After 15 UT, IMF By turned sharply to negative values, reaching −8 nT, and then again to the positive ones with the new peak of 20 nT around 18 UT.Kamide and Kusano (2015) reported that this severe geomagnetic storm (G4 level) was a result from the superposition of two successive, moderate storms, driven by two successive, southward IMF structures. The intense geomagnetic storm on 17–18 March 2015 leads to the auroral particle precipitation and an enhancement of the sub storm activity.

Scintillation index, Occurrence of Amplitude Scintillation (S4): Figure 2 shows different plots for amplitude scintillation index observed from 11th march to 19th march 2015.As shown in the graph, we are getting the scintillation activity before the storm. From the graph of March 10, we can see that the scintillation activity was very high from 2 pm to 4 pm, about 0.9. Next we also did strong scintillation activity observed on 13th and 14th of March but no activity was noticed on the day of the storm.If we look at the graph of 17th March then on the day when there was storm, scintillation activity was found to be very useful in which maximum value is 0.2 noticed.

Occurrence of Phase scintillation Index (Φ): Figure 3 shows different plots for amplitude scintillation index observed from 11th march to 19th march 2015.As shown in the graph, we are getting the scintillation activity before the storm. From the graph of March 10, we can see that the scintillation activity was very high from 2 pm to 4 pm, near about 1.

Figure 2. S4 activities during the sub storm activityfrom 11th march to 19th march 2015 over Darwin station Australia

Next we also did high scintillation activity observed on 12th, 13th and 14th of March but there is small activity was noticed on the day of the storm and its next days. If we look at the graph of 17th, 18th and 19th march scintillation activities goes down, scintillation activity was found to be very useful in which maximum value is 0.2 noticed.

DISCUSSION

In general, scintillation is believed to be strongly influenced by local time, season, solaractivity, geomagnetic conditions, and wave propagation from the underlying atmosphere.

The coronal mass ejections and solar wind interaction with the earth's magnetosphere cancause severe ionospheric irregularities by introducing scintillations in the signals throughplasma depletions associated with the equatorial plasma bubbles (EPBs) [1]. Geomagneticstorms may occur during the southward polarity of the interplanetary magnetic field (Bz) that manipulates the regular equatorial electric fields to trigger pre-reversal enhancements (PREs) to seed the generation and development of plasma bubbles [2–4]. During southward polarity of the interplanetary magnetic field (Bz) that manipulates the field, geomagnetic storms may occur. Also, the substorms formed at the polar authorizations can alter the tropical electric field during the recovery of geomagnetic storms performing in an increase or drop in the scintillation exertion (5 – 8).

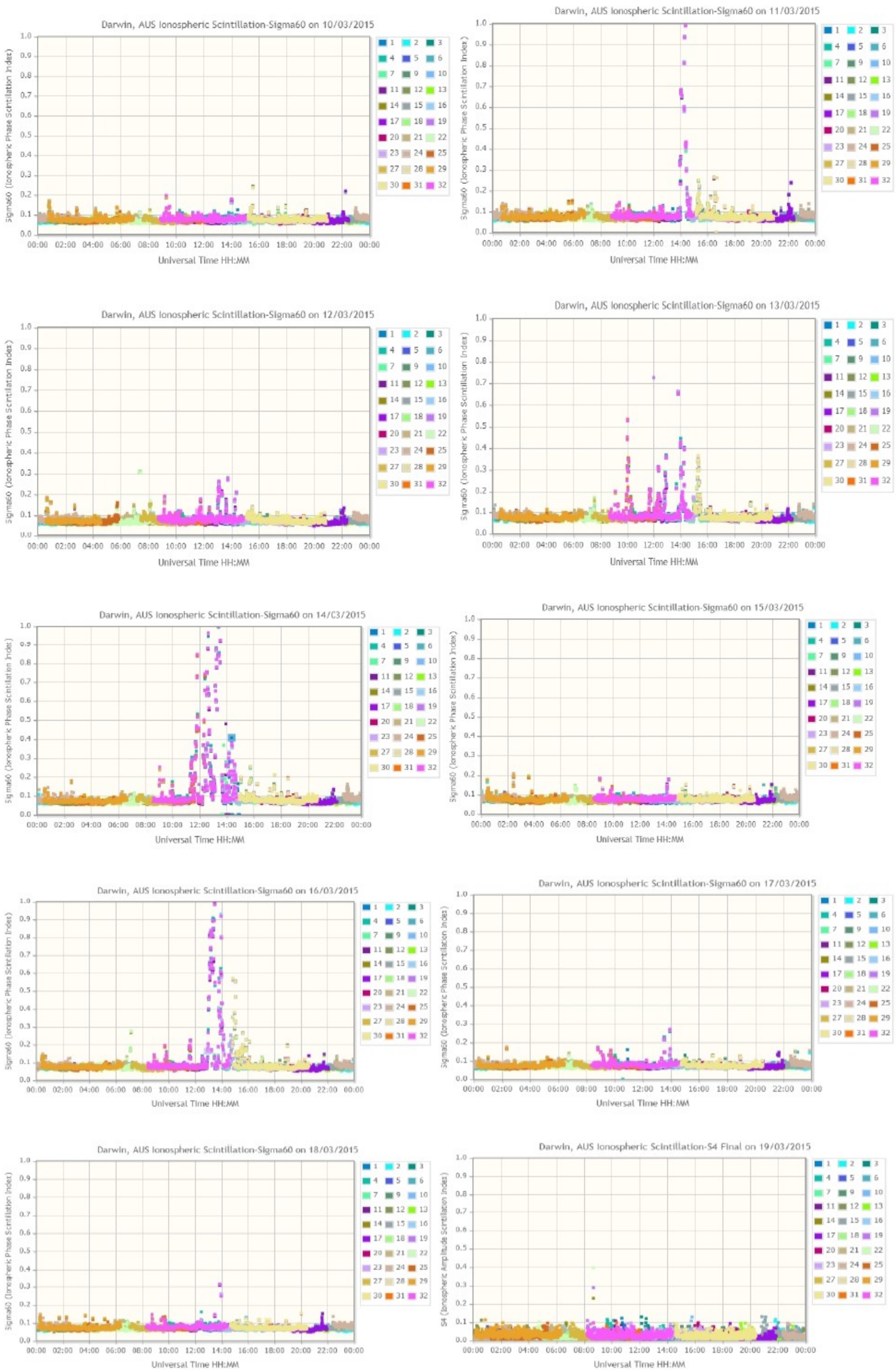

Figure 3. Phase Scintillation Index activities during the sub storm activity from 11th march to 19th march 2015 over Darwin station Australia

Generally, the ionospheric electrodynamics during the geomagnetic storms are affected by two sources (1) the short-lived piercing electric fields from high to low authorizations corresponding to the southward turning of the interplanetary glamorous field Bz to drive eastward (westward) the concentrated disturbances at the day and evening sectors (nightside) (9 – 12); and (2) the disturbance fireball electric fields performing from the changes in neutral winds that develop a many hours after the onset of the storm and generally last for several hours via thermospheric wind fireball action, frequently dominating in the recovery phase ().

It has been observed that during an extended main phase of the storm, the prompt penetration phase may coincide with the original dusk-time PRE at the tropical ionosphere to compound thepost-sunset ionospheric irregularities, indeed if this occurs with the concurrence of disturbance fireball electric fields (15). The disturbance fireball electric fields play an important part in the circumstance of day irregularities during the recovery phase of a storm (16) and references therein. It has been established that the scintillations are more frequent during the solar maximum times in the tropical and auroral regions, whereas their circumstances are meager in themid-latitudes . In the tropical regions, the scintillations are more prominent in thepost-sunset and night hours due to the circumstance of tube bubbles (19 – 21). Still, there are also shreds of substantiation for day scintillations, substantially associated with the sporadic-E (Es) structures, whose goods are fairly mild and less frequent, compared to the night- time scintillations . The scintillations are quantified in terms of two introductory measurable amounts, videlicet the breadth scintillation indicator (S4 indicator) and phase scintillation indicator (σ or Φ).

In GNSS operations, breadth scintillations relate to the rapid-fire oscillations in the signal intensity (or carrier-to- noise rate) measured by the receiver, whereas phase scintillation refers to the rapid-fire change in the carrier- phase measures, determined by the standard divagation of the detrended carrier phase over a period . While severe scintillations can beget a loss of cinch in the GNSS receivers, frequently making it insolvable to calculate the position for a period, a less severe scintillation condition may degrade the positioning and navigation delicacy by adding query to the signal. In the case of the breadth scintillation, the signal strength is degraded performing in the possible loss of cinch to essay the reacquisition of the signal, whereas the phase scintillation introduces a cycle slip or indeed the loss of signal cinch by holding considerable quantum of time for the reacquisition of the signal (). Hence, the dynamic systems counting on the GNSS carrier phase shadowing measures are veritably much vulnerable to the scintillation conditions (26). Piecemeal from the breadth and phase scintillations, the intensity of ionospheric scintillations or TEC oscillations can be quantitatively described by another indicator, called the rate of TEC indicator (ROTI) (). The breadth and phase scintillation indicators are generally tried at a high frequence with a especially configured cost-effective GNSS receiver simply for space rainfall monitoring, whose vacuity is meager across any region.

Still, the fairly abundant ordinarynon-scintillation geodetic receivers tried at a lower frequence could give original ROTI estimates, which are inversely useful for understanding the ionospheric irregularities in the absence of ionospheric monitoring receivers (29 – 31). ROTI refers to the standard divagation of the rate of change of TEC (Spoilage), whose values per nanosecond can be attained from the slant TEC estimations following the dispersive nature of refractive ionospheres in the binary- frequence phase and pseudorange observables. Over the last two decades, the expansive analysis of scintillation indicators and ROTI variations demonstrated a close relationship among the parameters (). Hence, it has been used by several ionospheric groups to dissect the TEC oscillations from an acceptable number of GNSS stations across the globe. Also, the coming generation transnational GNSS service (IGS) ROTI maps product can serve as a precious tool for covering global ionospheric irregularities and redefining the impact of tube irregularities on the GNSS positioning in the history (34).

CONCLUSION

In this study, the ionospheric scintillation occurrence during the geomagnetic storm event 17 march 2015 were investigated over the Darwin, Australia Scintillations which occurred during the disturbed period indicate the occurrence of equatorial plasma bubbles. The key findings are as follows:

1. The sudden storm commencement (SSC) was a quick drop of the SYM-H index to the value of −226 nT
2. The planetary index of the geomagnetic activity Kp reached the maximum value
3. During the main phase of the storm (17 March), the interplanetary magnetic field (IMF) orientation displayed a highly complex behavior.
4. The occurrence of phase scintillation activities was high before the storm period as compare with amplitude scintillation

REFERENCES

Knight, M.F. Ionospheric Scintillation Effects on Global Positioning System Receivers. Ph.D. Thesis, The University of Adelaide, Adelaide, Australia, December 2000.

Conker, R.S.; El Arini, M.B.; Hegarty, C.J.; Hsiao, T. Modeling the effects of ionospheric scintillation on GPS/Satellite-Based Augmentation System availability. Radio Sci. 2003, 38.

Elmas, Z.G.; Aquino, M.; Forte, B. The impact of ionospheric scintillation on the GNSS receiver signal tracking performance and measurement accuracy. In Proceedings of the 2011 XXXth URSI General Assembly and Scientific Symposium, Istanbul, Turkey, 13–20 August 2011; pp. 1–4.

Humphreys, T.E.; Psiaki, M.L.; Kintner, P.M. Modeling the effects of ionospheric scintillation on GPS carrier phase tracking. IEEE Trans. Aerosp. Electron. Syst. 2010, 46, 1624–1637.

Hofmann-Wellenhof, B.; Lichtenegger, H.; Collins, J. Global Positioning System: Theory and Practice; Springer: Berlin, Germany, 2012.

He, Z.; Zhao, H.; Feng,W. The Ionospheric Scintillation Effects on the BeiDou Signal Receiver. Sensors 2016, 16, 1883.

Beach, T.L.; Kintner, P.M. Development and use of a GPS ionospheric scintillation monitor. IEEE Trans. Geosci.Remote Sens. 2001, 39, 918–928.

Li, G.; Ning, B.; Hu, L.; Liu, L.; Yue, X.; Wan, W.; Zhao, B.; Igarashi, K.; Kubota, M.; Otsuka, Y. Longitudinaldevelopment of low-latitude ionospheric irregularities during the geomagnetic storms of July 2004.J. Geophys. Res. Space Phys. 2010, 115, 507–512.

Li, G.; Zhao, B.; Liu, L.; Wan, W.; Ding, F.; Liu, J.Y.; Ning, B.; Xu, J.S.; Yumoto, K.; Li, C. Characterizingthe 10 November 2004 storm-time middle-latitude plasma bubble and ionospheric scintillation event inSoutheast Asia. J. Geophys. Res. Atmos. 2009, 114.

Xu, R.; Liu, Z.; Li, M.; Morton, Y.; Chen, W. An analysis of low-latitude ionospheric scintillation and itseffects on precise point positioning. J. Glob. Position Syst. 2012, 11, 22–32.

Meggs, R.W.; Mitchell, C.N.; Honary, F. GPS scintillation over the European Arctic during the November2004 storms. GPS Solut. 2008, 12, 281–287.

Peymirat, C.; Kobea, A.T.; Richmond, A.D. Electrodynamic coupling of high and low latitudes: Simulations of shielding/

overshielding effects. J. Geophys. Res. Earth Surf. 2000, 105, 22991–23003. [CrossRef]

Blanc, M.; Richmond, A. The ionospheric disturbance dynamo. J. Geophys. Res. Earth Surf. 1980, 85, 1669–1686.

Fejer, B.G.; Larsen, M.F.; Farley, D.T. Equatorial disturbance dynamo electric fields. Geophys. Res. Lett. 1983, 10, 537–540.

Ram, S.T.; Rao, P.V.S.R.; Prasad, D.S.V.V.D.; Niranjan, K.; Krishna, S.G.; Sridharan, R.; Ravindran, S. Local time dependent response of postsunset ESF during geomagnetic storms. J. Geophys. Res. Earth Surf. 2008, 113.

Luo, W.; Xiong, C.; Xu, J.; Zhu, Z.; Chang, S. The Low-Latitude Plasma Irregularities after Sunrise from Multiple Observations in Both Hemispheres during the Recovery Phase of a Storm. Remote Sens. 2020, 12, 2897.

Klobuchar, J.A. Ionospheric Effects on GPS. In Global Positioning System: Theory and Applications; Parkinson, B.W., Spilker, J.J., Eds.; American Institute of Aeronautics & Astronautics: Reston, VA, USA, 1996; Volume 1, pp. 485–515.

Klobuchar, J.A.; Doherty, P.H. A Look Ahead: Expected Ionospheric Effects on GPS in 2000. GPS Solut. 1998, 2, 42–48.

Smith, J.; Heelis, R.A. Equatorial plasma bubbles: Variations of occurrence and spatial scale in local time, longitude, season, andsolar activity. J. Geophys. Res. Space Phys. 2017, 122, 5743–5755.

Okoh, D.; Rabiu, B.; Shiokawa, K.; Otsuka, Y.; Segun, B.; Falayi, E.; Onwuneme, S.; Kaka, R. First Study on the OccurrenceFrequency of Equatorial Plasma Bubbles over West Africa Using an All-Sky Airglow Imager and GNSS Receivers. J. Geophys. Res.Space Phys. 2017, 122, 12–430.

Gurav, O.; Sripathi, S.; Ghodpage, R. Radio and optical investigations of storm time evolution of post-midnight equatorial plasmabubbles (EPBs) and their drifts over Indian sector. Adv. Space Res. 2021, 67, 87–101.

Joshi, L.M.; Patra, A.K.; Pant, T.K.; Rao, S.V.B. On the nature of low-latitudeEsinfluencing the genesis of equatorial plasma bubble.J. Geophys. Res. Space Phys. 2013, 118, 524–532.

Seif, A.; Tsunoda, R.T.; Abdullah, M.; Hasbi, A.M. Daytime gigahertz scintillations near magnetic equator: Relationship toblanketing sporadic E and gradient-drift instability. Earth Planets Space 2015, 67, 177.

Bhattacharyya, A.; Beach, T.L.; Basu, S.; Kintner, P.M. Nighttime equatorial ionosphere: GPS scintillations and differential carrierphase fluctuations. Radio Sci. 2000, 35, 209–224.

Luo, X.; Gu, S.; Lou, Y.; Cai, L.; Liu, Z. Amplitude scintillation index derived from C/N0 measurements released by commongeodetic GNSS receivers operating at 1 Hz. J. Geodesy 2020, 94, 27.

Goodman, J.L.; Kramer, L. Scintillation Effects on Space Shuttle GPS Data. In Proceedings of the 2001 National Technical Meetingof The Institute of Navigation, Long Beach, CA, USA, 22–24 January 2001; pp. 742–752.

Bolaji, O.; Adebiyi, S.; Fashae, J. Characterization of ionospheric irregularities at different longitudes during quiet and disturbedgeomagnetic conditions. J. Atmos. Sol.-Terr. Phys. 2019, 182, 93–100

Pi, X.; Mannucci, A.J.; Lindqwister, U.J.; Ho, C.M. Monitoring of global ionospheric irregularities using the Worldwide GPSNetwork. Geophys. Res. Lett. 1997, 24, 2283–2286.

Olwendo, J.O.; Cilliers, P.; Weimin, Z.; Ming, O.; Yu, X. Validation of ROTI for Ionospheric Amplitude Scintillation Measurementsin a Low-Latitude Region Over Africa. Radio Sci. 2018, 53, 876–887.

Li, C.; Hancock, C.M.; Hamm, N.A.S.; Veettil, S.V.; You, C. Analysis of the Relationship between Scintillation Parameters,Multipath and ROTI. Sensors 2020, 20, 2877.

Gogie, T.K. The Rate of Ionospheric Total Electron Content Index (ROTI) as a Proxy for Nighttime Ionospheric Irregularity UsingEthiopian Low-Latitude GPS Data. Geomagn. Aeron. 2021, 61, 464–475.

Kotulak, K.; Zakharenkova, I.; Krankowski, A.; Cherniak, I.; Wang, N.; Fron, A. Climatology Characteristics of IonosphericIrregularities Described with GNSS ROTI. Remote Sens. 2020, 12, 2634.

****